Form factors for a proximity interaction between deformed nuclei

B. F. Bayman
School of Physics and Astronomy, University of Minnesota, Minneapolis, Minnesota 55455
(Received 3 February 1986)

A method is presented for the calculation of form factors for the interaction of two axially symmetric deformed nuclei via a proximity-plus-Coulomb potential. A distorted-wave Born approximation calculation for the inelastic scattering of 150 MeV ^{24}Mg from ^{154}Sm indicates that the proximity and centerline interactions produce significantly different M-substate populations in the final nuclear states.

I. INTRODUCTION

When two nonspherical nuclei approach each other, their interaction has both central and noncentral components. The so-called "centerline" potential depends only on the distance between the nuclear surfaces, measured along the line connecting their centers. It has a noncentral component if either or both nuclei are nonspherical, because then the centerline distance between the surfaces depends upon the orientation of the nuclei as well as upon the between-center distance. This orientation dependence of interaction energy implies the presence of internuclear torques: a torque will be exerted on each nonspherical nucleus, and we have the possibility of exchange of angular momentum between the relative and orientation degrees of freedom.

A possible limitation of the centerline potential is that its value is unaffected by rotation of the nuclei around the centerline, since such a rotation does not change the distance between the nuclear surfaces along the centerline. A consequence of this rotation invariance is the statement that the torque each nucleus exerts on the other has no component along the centerline.

Blocki *et al.*[1] have described a nucleus-nucleus "proximity" interaction whose properties can be derived from general considerations concerning the energy density of nuclear matter. This interaction is a function of the distance between the nuclear surfaces along the *shortest* line connecting the surfaces, which is not, in general, the line between centers. The proximity interaction also depends upon the shape of the gap between the surfaces in the vicinity of this shortest line. The gap shape changes if the nuclei are rotated about this line, and thus the torque each nucleus exerts on the other has a component along this line (and along the centerline). It might be expected that the presence of this torque component would have an effect on the relative populations of M-substate components in an inelastic collision of deformed nuclei.

References 2 and 3 have discussed the geometrically simpler situation in which one of the nuclei is spherical. In Ref. 2, a study was made of the difference between the strengths of the centerline and proximity potentials, as a function of the angle between the symmetry axis of the deformed nucleus and the relative vector between nuclear centers. A multipole analysis of this difference suggested that the two potentials would have significantly different effects when the angular momentum transfer is greater than or equal to four. This was confirmed in Ref. 3, by a coupled-channel calculation of data for ^{152}Sm(^{16}O,^{16}O$'$)^{152}Sm(4^+). It was found that the use of the proximity potential yielded a $\beta_4 R^4$ value consistent with results obtained by Coulomb excitation and electron scattering, whereas the centerline-potential analysis of the data required a $\beta_4 R^4$ value only half as large. It should be noted that in this case, with one nucleus spherical, neither the proximity potential nor the centerline potential leads to a torque component along the centerline. For this reason, we may expect even greater differences between the effects of the two potentials when both nuclei are deformed, since then the proximity potential implies a torque component along the centerline, whereas the centerline potential does not.

The first step in the calculation of the differential cross section for inelastic scattering produced by a particular interaction is the calculation of the radial form factors. These are matrix elements of the interaction with respect to the initial and final nuclear states, integrated over the internal degrees of freedom. In the present context, these internal degrees of freedom are the orientation degrees of freedom of the two deformed nuclei. In the following sections we will describe a method for calculating radial form factors for a proximity interaction and for a doubly folded Coulomb interaction between axially symmetry nuclei. We will then use these form factors in a distorted-wave Born approximation (DWBA) calculation to compare M-substate populations produced by proximity and centerline interactions.

II. THE FORM FACTORS

We consider the collision of two even-even nuclei. Each is assumed to be axially symmetric, and invariant[4] under a 180° rotation about an axis perpendicular to the symmetry axis. We assume that the nuclei remain in their $K=0^+$ ground-state rotational bands throughout the collision, with constant intrinsic states. Thus only their orientation degrees of freedom are affected by the collision. These orientation degrees of freedom are simply the spherical polar coordinates of the symmetry axes. Each nucleus can be in rotational states with angular mo-

menta $0^+,2^+,4^+,\ldots$. The normalized orientation wave function of nucleus i $(=1,2)$ when it has total angular momentum I_i and angular-momentum z component M_i is simply the spherical harmonic $Y^{I_i}_{M_i}(\theta_i\phi_i)$. Figure 1 represents the two nuclei at an instant when their axes have orientations θ_i,ϕ_i, and the line connecting their centers has orientation θ,ϕ and length r. The total scattering wave function can be expanded in the form

$$\Psi=\sum_{\substack{J\\S,l\\I_1,I_2}} u_{I_1I_2SlJ}(r)\{[Y^{I_1}(\theta_1\phi_1)Y^{I_2}(\theta_2\phi_2)]^S Y^l(\theta\phi)\}^J_0 . \quad (1)$$

The term shown in (1) has total angular momentum J, channel spin S, relative orbital angular momentum l, and parity $(-1)^l$.

The Schrödinger equation can be formulated[5] in terms of a set of coupled ordinary differential equations for the radial functions $u_{I_1I_2SlJ}(r)$. The coupling terms in this set are the following matrix elements:

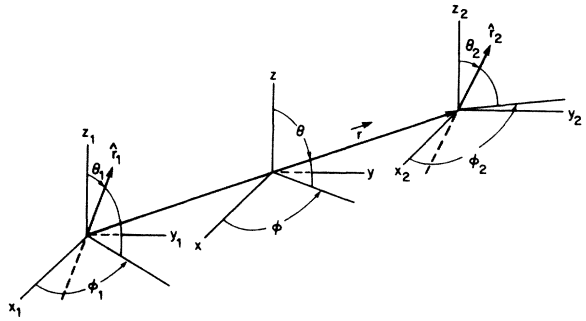

FIG. 1. $\hat{\mathbf{r}}_1$ and $\hat{\mathbf{r}}_2$ point along the axes of two axially symmetric nuclei, whose centers are separated by r. The orientations of $\hat{\mathbf{r}}_1$, $\hat{\mathbf{r}}_2$, and $\hat{\mathbf{r}}$ are specified by polar coordinates defined with respect to parallel sets of Cartesian axes.

$$\langle\{[Y^{I_1}(\theta_1\phi_1)Y^{I_2}(\theta_2\phi_2)]^S Y^l(\theta\phi)\}^J_0 \,|\, V(\theta_1\phi_1;\theta_2\phi_2;\theta\phi r) \,|\, \{[Y^{I_1'}(\theta_1\phi_1)Y^{I_2'}(\theta_2\phi_2)]^{S'} Y^{l'}(\theta\phi)\}^J_0\rangle \equiv F^J_{I_1I_2Sl,I_1'I_2'S'l'}(r) . \quad (2)$$

$V(\theta_1\phi_1;\theta_2\phi_2;\theta\phi r)$ in (2) is the interaction energy when the nuclei are in the configuration shown in Fig. 1. The integrations implied by this matrix element are over the six angles $\theta_1\phi_1\theta_2\phi_2\theta\phi$, for fixed values of the separation r. Because V is invariant under rotation of the entire system, the states in the bra and ket of (2) must have the same total angular momentum J if the matrix element is to be nonzero. Similarly, inversion invariances of V requires that the bra and ket have the same parity, which implies that l and l' differ by an even integer.

By using some straightforward angular momentum recoupling, we can express the matrix elements (2) in terms of "reduced" matrix elements $f_{L_1L_2L}(r)$, which depend upon fewer parameters:

$$F^J_{I_1I_2Sl,I_1'I_2'S'l'}(r)=\sum_{\substack{L\\L_1L_2}} [(Sl)_J(S'l')_{J'} \,|\, (SS')_L(ll')_L]_0[(I_1I_2)_S(I_1'I_2')_{S'} \,|\, (I_1I_1')_{L_1}(I_2I_2')_{L_2}]_L$$

$$\times(I_1I_1'00 \,|\, L_10)(I_2I_2'00 \,|\, L_20)(ll'00 \,|\, L0)i^{I_1+I_1'-L_1+I_2+I_2'-L_2+l+l'-L}$$

$$\times\left[\frac{(2I_1+1)(2I_1'+1)(2I_2+1)(2I_2'+1)(2l+1)(2l'+1)}{(4\pi)^3(2L_1+1)(2L_2+1)(2L+1)}\right]^{1/2} f_{L_1L_2L}(r) , \quad (3a)$$

$$f_{L_1L_2L}(r)=\int \sin\theta_1 d\theta_1 d\theta_1 \int \sin\theta_2 d\theta_2 d\phi_2 \int \sin\theta\, d\theta\, d\phi\, V(\theta_1\phi_1;\theta_2\phi_2;\theta\phi r)\{[Y^{L_1}(\theta_1\phi_1)Y^{L_2}(\theta_2\phi_2)]^L Y^L(\theta\phi)\}^0_0 . \quad (3b)$$

The parameter L has the significance of the angular momentum transferred between the internal (i.e., nuclear axis orientation) and relative motion. Similarly, L_i $(i=1,2)$ has the significance of the angular momentum transferred to nucleus i. The main concern of this paper is the evaluation of the "form factor" (3b). The techniques to be used for the nuclear and Coulomb interactions are different, and so we will discuss them in turn.

A. Nuclear interaction

Since the integrand in (3b) is rotationally invariant, its value is unchanged if $\hat{\mathbf{r}}_1$, $\hat{\mathbf{r}}_2$, and $\hat{\mathbf{r}}$ in Fig. 1 are simultaneously subjected to the same rotation. Thus if we replace the six angles $\theta_1\phi_1\theta_2\phi_2\theta\phi$ by three intrinsic angles and three overall orientation angles, the integrand will be independent of the overall orientation angles. The intrinsic angles are defined as shown in Fig. 2, with $\hat{\mathbf{r}}$ along the $\hat{\mathbf{z}}$ axis and $\hat{\mathbf{r}}_1$ in the x-z plane with $(\hat{\mathbf{r}})_x>0$. Clearly, any configuration of $\hat{\mathbf{r}}_1$, $\hat{\mathbf{r}}_2$, and $\hat{\mathbf{r}}$ can be obtained from three vectors oriented as shown in Fig. 2, by means of an overall rotation which does not affect the value of the integrand in (3b). The integration over these overall orientation coordinates simply gives a factor of $8\pi^2$, and (3b) becomes

$$f_{L_1L_2L}(r)=8\pi^2\int_{\theta_1=0}^{\pi}\sin\theta_1 d\theta_1\int_{\theta_2=0}^{\pi}\sin\theta_2 d\theta_2\int_{\phi_2=-\pi}^{\pi}d\phi_2 V(\theta_1 0;\theta_2\phi_2;00r)\{[Y^{L_1}(\theta_1 0)Y^{L_2}(\theta_2\phi_2)]^L Y^L(00)\}_0^0 . \quad (4)$$

It is convenient to express the spherical harmonics in terms of reduced Wigner d functions,[6]

$$Y_m^l(\theta\phi)=i^l\left[\frac{2l+1}{4\pi}\right]^{1/2}e^{im\phi}d_{m,0}^l(\theta) , \quad (5a)$$

$$d_{m,0}^l(\theta)=\sum_n(-1)^n\frac{l!\sqrt{(l-m)!(l+m)!}}{n!(l+m-n)!(l-n)!(n-m)!}\left[\cos\frac{\theta}{2}\right]^{2l+m-2n}\left[\sin\frac{\theta}{2}\right]^{2n-m}=(-1)^m d_{-m,0}^l(\theta) , \quad (5b)$$

so that (4) becomes

$$f_{L_1L_2L}(r)=i^{L_1+L_2-L}\sqrt{\pi(2L_1+1)(2L_2+1)}\sum_m(-1)^m(L_1L_2m-m\mid L0)$$
$$\times\int_0^{\pi}\sin\theta_1 d\theta_1\int_0^{\pi}\sin\theta_2 d\theta_2\int_{-\pi}^{\pi}d\phi_2 e^{-im\phi_2}d_{m,0}^{L_1}(\theta_1)d_{m,0}^{L_2}(\theta_2)V(\theta_1 0;\theta_2\phi_2;00r) . \quad (6)$$

Because we have assumed that each nucleus is invariant under rotation about its body-fixed y axis, V in (3b) is unchanged if $(\theta_1\phi_1)$ is replaced by $(\pi-\theta_1,\pi+\phi_1)$ or if $(\theta_2\phi_2)$ is replaced by $(\pi-\theta_2,\pi+\phi_2)$. Since these operations multiply the respective spherical harmonics by $(-1)^{L_1}$ and $(-1)^{L_2}$, the integral (3b) vanishes unless L_1 and L_2 are even. Similarly, V is unchanged if all three directions $\hat{\mathbf{r}}_1,\hat{\mathbf{r}}_2,\hat{\mathbf{r}}$ are simultaneously inverted (this is the parity operation). Thus it also follows that L is even. This means that the vector-coupling coefficient in (6) is unchanged if m is replaced by $-m$, and we can use (5b) to restrict the sum in (6) to non-negative m values:

$$f_{L_1L_2L}(r)=i^{L_1+L_2-L}2\sqrt{\pi(2L_1+1)(2L_2+1)}\sum_{m\geq 0}(-1)^m\frac{(L_1L_2m-m\mid L0)}{1+\delta_{m,0}}$$
$$\times\int_0^{\pi}\sin\theta_1 d\theta_1\int_0^{\pi}\sin\theta_2 d\theta_2\int_{-\pi}^{\pi}d\phi_2 d_{m,0}^{L_1}(\theta_1)d_{m,0}^{L_2}(\theta_2)\cos(m\phi_2)$$
$$\times V(\theta_1 0;\theta_2\phi_2;00r) . \quad (7)$$

In addition, inspection of Fig. 2 shows that replacing ϕ_2 by $-\phi_2$ simply produces a reflection of the system across the x-z plane, which has no effect on V. Thus the ϕ_2 integration range can be restricted to $0\leq\phi_2\leq\pi$. Furthermore, V is obviously unchanged if both nuclei in Fig. 2 are rotated by π around the z axis. If we combine this rotation with rotations of both nuclei about their intrinsic y axes, we see that

$$V(\theta_1 0;\theta_2\phi_2;00r)=V(\pi-\theta_1,0;\pi-\theta_2,\phi_2;00r) . \quad (8a)$$

Finally, invariance of V under inversion of $\hat{\mathbf{r}}_2$ and reflection of $\hat{\mathbf{r}}_2$ across the x-z plane, yields

$$V(\theta_1 0;\theta_2\phi_2;00r)=V(\theta_1 0;\pi-\theta_2,\pi-\phi_2;00r) . \quad (8b)$$

Equations (8a) and (8b), and the fact that L_1 and L_2 are even, enable us to restrict the θ_1 and θ_2 integrations in (7) to the range $0\leq\theta_1,\theta_2\leq\pi/2$. The final result can be written

$$f_{L_1L_2L}(r)=i^{L_1+L_2-L}16\sqrt{\pi(2L_1+1)(2L_2+1)}\sum_{m\geq 0}\frac{(-1)^m(L_1L_2m-m\mid L0)}{1+\delta_{m,0}}$$
$$\times\int_0^1 dx_1\int_0^1 dx_2\int_0^{\pi}d\phi_2 d_{m,0}^{L_1}(\theta_1)d_{m,0}^{L_2}(\theta_2)\cos(m\phi_2)V(\theta_1 0;\theta_2\phi_2;00r) , \quad (9)$$

with $\theta_1=\arccos(x_1)$ and $\theta_2=\arccos(x_2)$.

To perform a numerical evaluation of the integral in (9), we must be able to calculate the interaction between the nuclei for any separation and orientations. If we use the proximity potential, this requires us to determine the length d of the shortest line between the nuclear surfaces, and the principal radii of curvature R_1,R_2, of the gap at the location of this shortest line. In terms of these quantities, the proximity interaction[1] is

$$V=4\pi\gamma\bar{R}b\Phi(\zeta),\quad R=\sqrt{R_1R_2},\quad \zeta=d/b . \quad (10a)$$

The function Φ and the parameters b and γ are taken to be

$$\Phi(\zeta\leq\zeta_1)=\tfrac{1}{2}(\zeta-\zeta_0)^2-k(\zeta-\zeta_0)^3 ,$$
$$\Phi(\zeta>\zeta_1)=-3.347\exp(-\zeta/0.75) , \quad (10b)$$
$$\zeta_1=1.254,\quad \zeta_0=2.54,\quad k=0.0852 .$$

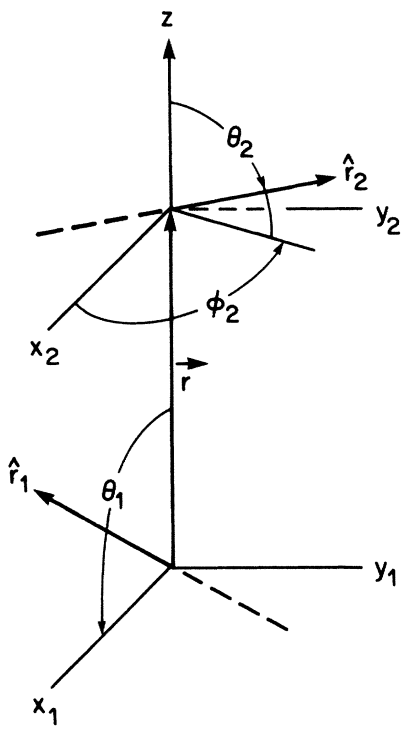

FIG. 2. The nuclear configuration of Fig. 1 rotated so that $\hat{\mathbf{r}}$ coincides with the $\hat{\mathbf{z}}$ axis, and $\hat{\mathbf{r}}_1$ lies in the x-z plane with $(\hat{\mathbf{r}})_x > 0$.

Figure 3 shows the iterative procedure used to locate the points on the nuclear surfaces at opposite ends of the shortest line between them. This line will be perpendicular to the two surfaces where it meets them, and (for axially symmetric nuclei) will intersect their symmetry axes. The iteration begins at the center of nucleus 1 (point A). A line is then drawn through A, perpendicular to the surface of nucleus 2. This line is extended until it reaches the axis of nucleus 2 (point B). From B, a line is drawn perpendicular to the surface of nucleus 1, and extended until it reaches the axis of nucleus 1 (point C). This across-and-back procedure is repeated until the distance between two successive intersections with the axis of nucleus 1 is less than some preassigned tolerance (chosen to be 0.001 fm for the calculations presented in the next section).

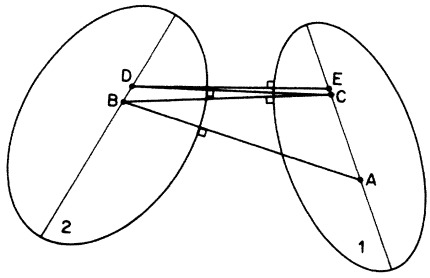

FIG. 3. Line AB is drawn from A perpendicular to the surface of nucleus 2, line BC is drawn from B perpendicular to the surface of nucleus 1, etc. The closeness of points E and C indicates convergence to the line perpendicular to both surfaces.

Once this shortest line between the surfaces is located, d and $\overline{R}$ can be calculated for axially symmetric nuclei of arbitrary shape using the formulae given in Sec. V of Ref. 3.

B. Coulomb interaction

In this case, the interaction V in (3b) is a double volume integral over the two nuclei:

$$V(\theta_1\phi_1;\theta_2\phi_2;\theta\phi r) = \int d^3r_1 d^3r_2 \frac{P_{\phi_1\theta_1 0}\rho_1(\mathbf{r}_1)P_{\phi_2\theta_2 0}\rho_2(\mathbf{r}_2)}{|r\hat{\mathbf{r}}(\theta\phi)+\mathbf{r}_2-\mathbf{r}_1|} \tag{11}$$

(see Fig. 4). Here, $\rho_i(\mathbf{r}_i)$ represents the charge density of nucleus i in its own body-fixed coordinate system. Thus ρ_i is an axially symmetric function and can be expanded in terms of Legendre polynomials,

$$\rho_i(r,\alpha)=\sum_l u_l^{(i)}(r)P_l(\cos\alpha)\ , \tag{12a}$$

$$u_l^{(i)}(r)=(2l+1)\int_0^1 \rho_i(r,\arccos(x))P_l(x)dx\ . \tag{12b}$$

$P_{\phi\theta 0}$ in (11) represents a rotation operator, so that $P_{\phi_i\theta_i 0}\rho_i(\mathbf{r}_i)$ is the charge density at $\mathbf{r}_i$ when nucleus i is rotated so that its symmetry axis has polar coordinates θ_i,ϕ_i. If (11) is used in (3b), we obtain

$$f^{\text{Coul}}_{L_1L_2L}(r)=\int \sin\theta_1 d\theta_1 d\phi_1 \int \sin\theta_2 d\theta_2 d\phi_2 \int \sin\theta\, d\theta\, d\phi \{[Y^{L_1}(\theta_1\phi_1)Y^{L_2}(\theta_2\phi_2)]^L Y^L(\theta\phi)\}^0_0 \times \int d^3r_1 d^3r_2 \frac{P_{\phi_1\theta_1 0}\rho_1(\mathbf{r}_1)P_{\phi_2\theta_2 0}\rho_2(\mathbf{r}_2)}{|r\hat{\mathbf{r}}(\theta\phi)+\mathbf{r}_2-\mathbf{r}_1|}\ . \tag{13}$$

If we use the expansion (12), we can express the $\theta_i\phi_i$ integrals as

$$\int_{(\text{fixed } \mathbf{r}_i)} \sin\theta_i d\theta_i d\phi_i Y^{L_i}_{M_i}(\theta_i\phi_i)P_{\phi_i\theta_i 0}\rho_i(\mathbf{r}_i)=\frac{4\pi}{2L_i+1}u^{(i)}_{L_i}(r_i)Y^{L_i}_{M_i}(\hat{\mathbf{r}}_i)\equiv\frac{4\pi}{2L_i+1}\psi^{L_i}_{M_i}(\mathbf{r}_i)\ , \tag{14}$$

so that (13) becomes

$$f^{\text{Coul}}_{L_1L_2L}(r)=\frac{(4\pi)^2}{(2L_1+1)(2L_2+1)}\int \sin\theta\, d\theta\, d\phi \int d^3r_1 d^3r_2 \frac{\{[\psi^{L_1}(\mathbf{r}_1)\psi^{L_2}(\mathbf{r}_2)]^L Y^L(\theta\phi)\}^0_0}{|r\hat{\mathbf{r}}(\theta\phi)+\mathbf{r}_2-\mathbf{r}_1|}\ . \tag{15}$$

Because the denominator in (15) depends on $\mathbf{r}_2-\mathbf{r}_1$, it is convenient to do the integral using relative and center-of-mass coordinates:

$$\mathbf{R}'=\frac{\mathbf{r}_1+\mathbf{r}_2}{2},\quad \mathbf{r}'=\mathbf{r}_1-\mathbf{r}_2\ , \tag{16a}$$

$$\int d^3r_1 d^3r_2 \frac{[\psi^{L_1}(\mathbf{r}_1)\psi^{L_2}(\mathbf{r}_2)]^L_M}{|r\hat{\mathbf{r}}(\theta\phi)+\mathbf{r}_2-\mathbf{r}_1|}=\int d^3r' d^3R' \frac{[\psi^{L_1}(\mathbf{R}'+\mathbf{r}'/2)\psi^{L_2}(\mathbf{R}'-\mathbf{r}'/2)]^L_M}{|r\hat{\mathbf{r}}(\theta\phi)-\mathbf{r}'|}\ . \tag{16b}$$

The angular part of the $\mathbf{R}'$ integration yields a result of the form

$$\int d\hat{\mathbf{R}}'[\psi^{L_1}(\mathbf{R}'+\mathbf{r}'/2)\psi^{L_2}(\mathbf{R}'-\mathbf{r}'/2)]^L_M=\frac{1}{r'R'}g_{L_1L_2L}(r',R')Y^L_M(\hat{\mathbf{r}}')\ . \tag{17}$$

The radial function $g_{L_1L_2L}(r',R')$ in (17) can be calculated with the method used by Bayman and Kallio[7] to project out the relative $l=0$ part of two-particle shell-model wave functions. The result is

$$g_{L_1L_2L}(r',R')=i^{L_1+L_2-L}\left[\frac{\pi(2L_1+1)(2L_2+1)}{2L+1}\right]^{1/2} r'R'$$
$$\times\int_{x=-1}^{1} dx\, u_{L_1}(r'_1)u_{L_2}(r'_2)\sum_M (L_1L_2M-M\,|\,L0)d^{L_1}_{M,0}(\theta_1)d^{L_2}_{M,0}(\theta_2)\ , \tag{18a}$$

with

$$\left.\begin{matrix} r'_1 \\ r'_2 \end{matrix}\right\}=\left[\left[\frac{r'}{2}\right]^2+(R')^2\pm r'R'x\right]^{1/2}, \tag{18b}$$

$$\cos\theta_1=\frac{r'/2+R'x}{r_1},\quad \cos\theta_2=\frac{-r'/2+R'x}{r_2}\ . \tag{18c}$$

When (17) is used in (16b) and (15), the result is

$$f^{\text{Coul}}_{L_1L_2L}(r)=\frac{(4\pi)^2}{(2L_1+1)(2L_2+1)}\int \sin\theta\, d\theta\, d\phi \int d^3r' \frac{1}{|r\hat{\mathbf{r}}(\theta\phi)-\mathbf{r}'|}\int R'^2 dR' \frac{g_{L_1L_2L}(r',R')}{r'R'}[Y^L(\hat{\mathbf{r}}')Y^L(\theta\phi)]^0_0\ .$$

We then use a Slater expansion,

$$\frac{1}{|r\hat{\mathbf{r}}(\theta\phi)-\mathbf{r}'|}=\sum_L \frac{r^L_<}{r^{L+1}_>}\frac{4\pi}{\sqrt{2L+1}}[Y^L(\hat{\mathbf{r}}')Y^L(\theta,\phi)]^0_0\ , \tag{19}$$

to obtain our final result:

$$f^{\text{Coul}}_{L_1L_2L}(r)=\frac{(4\pi)^3}{(2L_1+1)(2L_2+1)\sqrt{2L+1}}\left[\frac{1}{r^{L+1}}\int_0^r h_{L_1L_2L}(r')(r')^{L+1}dr'+r^L\int_r^\infty h_{L_1L_2L}(r')(r')^{-L}dr'\right], \tag{20a}$$

$$h_{L_1L_2L}(r')\equiv\int_0^\infty R'dR' g_{L_1L_2L}(r',R')\ . \tag{20b}$$

Note that (20) is valid at *all* separations r; it is not limited to situations in which the charge distributions do not overlap during the integrations in (13).

Equations (9) and (20) were used to calculate the nuclear (proximity) and Coulomb contributions to the form factors (3b). The numerical calculations were performed at the Central Computing Facility of Los Alamos National Laboratory and at the University of Minnesota Supercomputing Institute.

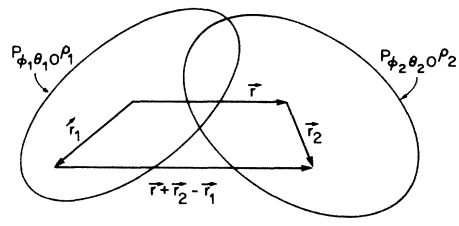

FIG. 4. Calculating the Coulomb interaction between the nuclei when they have orientations $\theta_1,\phi_1,\theta_2,\phi_2$. Note that these angles are kept fixed during the $\mathbf{r}_1,\mathbf{r}_2$ integrations.

III. A COMPARISON OF PROXIMITY AND CENTER-LINE INTERACTIONS

A complete discussion of the collision between axially symmetric deformed nuclei would require solutions of sets of coupled-channel equations,[5] with (3), (9), and (20) used to calculate the interaction matrix elements. At this time we will present a more modest calculation: a DWBA prediction for the simultaneous excitation of two deformed nuclei. Our object is to compare the effect of the proximity interaction (10) with that of the more commonly used centerline interaction.

Suppose two axially symmetric nuclei in their ground states make a direct inelastic transition to final $K=0^+$ states with angular momentum quantum numbers I_1M_1 and I_2M_2, respectively. The DWBA matrix element[8] is

$$F_{00\to I_1M_1,I_2M_2}(\mathbf{k}_i,\mathbf{k}_f)=\langle Y^{I_1}_{M_1}(\theta_1\phi_1)Y^{I_2}_{M_2}(\theta_2\phi_2)\chi^{(-)}(\mathbf{k}_f,\mathbf{r})\,|\,V(\theta_1\phi_1;\theta_2\phi_2;\theta\phi r)\,|\,Y^0_0(\theta_1\phi_1)Y^0_0(\theta_2\phi_2)\chi^{(+)}(\mathbf{k}_i,\mathbf{r})\rangle\ . \tag{21}$$

Here, $\chi^{(+)}$ and $\chi^{(-)}$ are distorted waves describing the relative motion. Writing out the integrals explicitly, we have

$$\begin{aligned}F_{00\to I_1M_1,I_2M_2}(\mathbf{k}_i,\mathbf{k}_f)&=\frac{1}{4\pi}\sum_L(I_1I_2M_1M_2\,|\,LM_1+M_2)\\&\times\int d^3r\,\chi^{(-)*}(\mathbf{k}_f,\mathbf{r})\left\{\int \sin\theta_1 d\theta_1 d\phi_1\sin\theta_2 d\theta_2 d\phi_2[Y^{I_1}(\theta_1\phi_1)Y^{I_2}(\theta_2\phi_2)]^{L*}_{M_1+M_2}V(\theta_1\phi_1;\theta_2\phi_2;\theta\phi r)\right\}\\&\times\chi^{(+)}(\mathbf{k}_i,\mathbf{r})\ .\end{aligned} \tag{22}$$

If we compare the quantity in curly braces in (22) with (3b), we see that

$$\int \sin\theta_1 d\theta_1 d\phi_1\sin\theta_2 d\theta_2 d\phi_2[Y^{I_1}(\theta_1\phi_1)Y^{I_2}(\theta_2\phi_2)]^{L*}_{M_1+M_2}V(\theta_1\phi_1;\theta_2\phi_2;\theta\phi r)=\frac{1}{\sqrt{2L+1}}f_{I_1I_2L}(r)Y^{L*}_{M_1+M_2}(\theta\phi)\ ,$$

so that (3b) is the form factor to be used in the DWBA matrix element:

$$F_{00\to I_1M_1,I_2M_2}(\mathbf{k}_i,\mathbf{k}_f)=\frac{1}{4\pi}\sum_L\frac{(I_1I_2M_1M_2\,|\,LM_1+M_2)}{\sqrt{2L+1}}\int d^3r\,\chi^{(-)*}(\mathbf{k}_f,\mathbf{r})f_{I_1I_2L}(r)Y^{L*}_{M_1+M_2}(\theta\phi)\chi^{(+)}(\mathbf{k}_i,\mathbf{r})\ . \tag{23}$$

We have chosen, as an example, the inelastic scattering of 150 MeV ^{24}Mg nuclei from ^{154}Sm, leading to simultaneous excitation of the 2^+ level of ^{24}Mg and the 4^+ level of ^{154}Sm. Each nucleus is represented by an axially symmetric spheroid whose shape in its body-fixed coordinate system is given by

$$R(\theta)=R_0\left[1+\sum_L i^{-L}\beta_L\,Y^L_0(\theta\phi)\right]\ . \tag{24}$$

We have used $R_0=3$ fm, $\beta_2=0.2$, and $\beta_4=0.1$ for ^{24}Mg, and $R_0=5$ fm, $\beta_2=0.1$, $\beta_4=0.05$, $\beta_6=0.025$, and $\beta_8=0.01$ for ^{154}Sm. These values should give a reasonable description of the nuclear shapes; they are not expected to be quantitatively exact. For the DWBA calculation we have used the same optical potentials in the initial and fi-

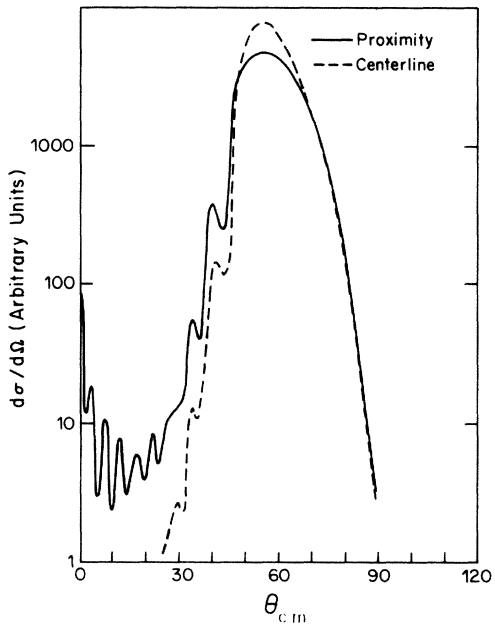

FIG. 5. DWBA cross sections for the simultaneous inelastic excitation of 2^+ and 4^+ levels in ^{24}Mg and ^{154}Sm, respectively. The same Coulomb interaction is used for the two curves, but the nuclear interaction is taken to be a proximity potential for the solid curve and a centerline potential for the dashed curve. The relative normalization of the two curves is arbitrary.

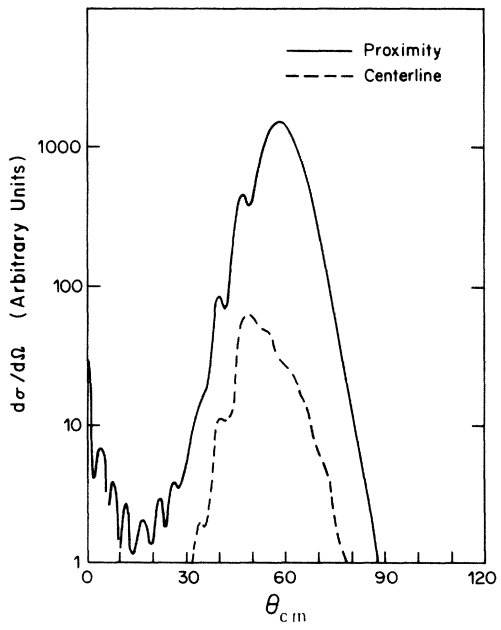

FIG. 6. The same as in Fig. 5, except that the only ^{24}Mg(2^+) states included are those with $M=\pm1$ (defined relative to an axis perpendicular to the reaction plane). The relative normalization of the two curves is the same as in Fig. 5.

nal channels: $V=-100$ MeV, $r_0=1.09$ fm, and $a=0.78$ fm for the real part, and $W=-20$ MeV, $r_I=1.27$ fm, and $a_I=0.6$ fm for the (volume) imaginary part. We have considered two nucleus-nucleus interactions: the Coulomb-plus-proximity interaction discussed above, and a Coulomb-plus-centerline interaction. This centerline interaction has the same distance dependence (10) as the proximity interaction, but the variable d is replaced by the distance between the nuclear surfaces along the line connecting the nuclear centers. Furthermore, the dependence of V on the gap radii of curvature is omitted. Figure 5 shows a comparison of the differential cross sections calculated with the DWBA program DWUCK,[9] using form factors calculated with these two interactions, and summed over all final M values. It is seen in Fig. 5 that both differential cross sections have the familiar shape of a broad maximum centered at the scattering angle of a grazing Coulomb orbit, on which is superimposed oscillatory structure associated with interference between orbits passing on opposite sides of the nuclei.[10] The relative normalizations of the two curves is chosen to make them nearly equal in the region of the Coulomb maximum. Figure 6 shows plots of the differential cross sections as measured by a detector sensitive only to the $M=\pm 1$ components of the ^{24}Mg 2^+ level, with these M components defined relative to an axis perpendicular to the reaction plane. Such a cross section could be measured, for example, by detecting only those events that were coincident with the emission of the deexcitation γ ray ($2^+\rightarrow 0^+$) perpendicular to the reaction plane.[11] The relative scale factor used in the proximity and centerline plots in Fig. 6 is the same as that used in Fig. 5. It is seen that the $M=\pm 1$ centerline differential cross section is more than an order of magnitude smaller than the $M=\pm 1$ proximity differential cross section, even though the differential cross sections summed over all M values are comparable. Thus, this DWBA calculation indicates that the distribution of flux between the final M states is strongly affected by the extra torque that the proximity interaction provides.

IV. DISCUSSION

A complete coupled-channel calculation for the inelastic scattering of axially deformed nuclei would be a very formidable task. If we decide to include rotational levels with angular momenta up to a maximum of I_m for each nucleus, the number of channels that must be coupled (i.e., the number of compatible I_1,I_2,l values) for total angular momentum J and parity π is

$$\frac{(I_m^2+2I_m+2)(I_m+2)^2}{8} \quad \text{if } \pi(-1)^J \text{ is even},$$

$$\frac{I_m(I_m+2)^3}{8} \quad \text{if } \pi(-1)^J \text{ is odd}.$$

Thus it is necessary to restrict I_m to a rather low value, or to use an approximate version of the coupled-channel formalism, such as the adiabatic approximation[12] or a calculation in which quantum effects are included in the treatment of the orientation degrees of freedom, but the relative motion of the two nuclei is treated classically.[13] An important ingredient in all these calculations is the choice of the interaction between the nuclei, and the determination of its radial form factors. The main object of this paper has been to present a convenient and practical procedure for the calculation of form factors for a proximity interaction. Moreover, a DWBA calculation indicates that proximity and centerline interactions can lead to observably different populations of final M substates. Any process which can be affected by the orientation of the two nuclei as they approach each other is probably sensitive to the details of the noncentral component of the nucleus-nucleus interaction.

[1] J. Blocki, J. Randrup, W. J. Swiatecki, and C. F. Tsang, Ann. Phys. (N.Y.) **105**, 427 (1977).

[2] J. Randrup and J. S. Vaagen, Phys. Lett. **77B**, 170 (1978).

[3] A. J. Baltz and B. F. Bayman, Phys. Rev. C **26**, 1969 (1982).

[4] A. Bohr and B. R. Mottelson, *Nuclear Structure* (Benjamin, New York, 1975), Vol. II, Chap. 4.

[5] See, for example, T. Tamura, Rev. Mod. Phys. **37**, 679 (1965); S. Landowne and A. Vitturi, *Treatise on Heavy-Ion Science* (Plenum, New York, 1984), Vol. 1, p. 355; G. R. Satchler, *Direct Nuclear Reactions* (Clarendon, Oxford, 1983), Chap. 5.

[6] E. P. Wigner, *Group Theory and Its Applications to the Quantum Mechanics of Atomic Spectra* (translated by J. J. Griffen) (Academic, New York, 1959), Chap. 15.

[7] B. F. Bayman and A. Kallio, Phys. Rev. **156**, 1121 (1967).

[8] G. R. Satchler, *Direct Nuclear Reactions*, Ref. 5, Chap. 6; N. Austern, *Direct Nuclear Reaction Theories* (Wiley-Interscience, New York, 1970), Chap. 4.

[9] D. R. Kunz (private communication).

[10] V. M. Strutinsky, Zh. Eksp. Teor. Fiz. **46**, 2078 (1964) [Sov. Phys.—JETP **19**, 1401 (1964)]; S. Kahana, P. D. Bond, and C. Chasman, Phys. Lett. **50B**, 199 (1974).

[11] W. Dunnweber, P. D. Bond, C. Chasman, and S. Kubono, Phys. Rev. Lett. **43**, 1642 (1979); F. H. Schmidt, R. E. Brown, J. B. Gerhart, and W. E. Kolasinski, Nucl. Phys. **52**, 353 (1964); W. Dunnweber, in *Spin Vector of Fragments in Deep Inelastic Reactions*, proceedings of the International School of Physics "Enrico Fermi," Course LXXXVII, 1984, edited by L. Moretto and R. A. Ricci (North-Holland, Amsterdam, 1984).

[12] T. Tamura, Rev. Mod. Phys. **37**, 689 (1965).

[13] K. Alder and A. Winther, *Electromagnetic Excitation* (North-Holland, Amsterdam, 1975); R. A. Broglia, G. Pollarolo, C. H. Dasso, and T. Dossing, Phys. Rev. Lett. **43**, 1649 (1979); R. A. Broglia, C. H. Dasso, and A. Winther, Coherent Surface Excitation Model of Heavy-ion Reactions, in *Proceedings of the International School of Physics "Enrico Fermi"*, Course LXXVII, 1981, edited by R. A. Broglia, R. A. Ricci, and C. H. Dasso (North-Holland, Amsterdam, 1981), p. 327.